

meta-Phosphonobenzoic Acid: A Rigid Heterobifunctional Precursor for the Design of Hybrid Materials

Jean-Michel Rueff,^{*[a]} Vincent Caignaert,^[a] Sophie Chausson,^[a] André Leclaire,^[a] Charles Simon,^[a] Olivier Perez,^[a] Loïc Le Pluart,^[b] and Paul-Alain Jaffrès^{*[c]}

Keywords: Phosphonates / Carboxylic acids / Hydrothermal synthesis / Acidity / Magnetic properties

Rigid *meta*-phosphonobenzoic acid **2** possesses two functional groups (phosphonic acid and carboxylic acid) both having the aptitude to associate with a metallic precursor to form hybrid materials. The hydrothermal reactions of compound **2** with $\text{MnCl}_2 \cdot 4\text{H}_2\text{O}$ or $\text{Co}(\text{NO}_3)_2 \cdot 6\text{H}_2\text{O}$ produce, respectively, the isostructural layered materials $\text{M}(\text{H}_2\text{O})_2(\text{PO}_3\text{C}_6\text{H}_4\text{CO}_2\text{H})$ (**3**, $\text{M} = \text{Mn}$; **4**, $\text{M} = \text{Co}$) characterized by the presence of the free carboxylic acid groups in the interlayer space (space group $P2_1/n$). The reaction of $\text{Zn}(\text{CH}_3\text{COO})_2 \cdot 2\text{H}_2\text{O}$ with **2** produces two different materials depending on the pH of the reaction media. At low pH (pH < 4.1), the iso-

structural material $\text{Zn}(\text{H}_2\text{O})(\text{PO}_3\text{C}_6\text{H}_4\text{CO}_2\text{H})$ (**5**) is formed possessing Zn^{II} atoms octahedrally coordinated. At higher pH, generated by the addition of urea in the hydrothermal reaction, $\text{Zn}_3(\text{H}_2\text{O})_2(\text{PO}_3\text{C}_6\text{H}_4\text{CO}_2)_2$ (**6**) is formed (orthorhombic; space group $P\text{can}$). In material **6**, the phosphonic acid and the carboxylic acid groups are linked to the inorganic network. One of the two Zn^{II} centres is tetrahedrally coordinated and the other is surrounded by a trigonal bipyramid.

(© Wiley-VCH Verlag GmbH & Co. KGaA, 69451 Weinheim, Germany, 2008)

Introduction

Metal–organic frameworks (MOFs) or coordination networks,^[1] synthesized from the reaction involving organic molecules and metallic salts, have attracted much interest in recent years owing to their potential applications in different areas including gas storage,^[2] catalysis,^[3] chiral separation,^[4] nonlinear optical materials^[5] or drug storage.^[6] The rigidity of the organic precursor has a great influence on the shape of the hybrid materials. For this reason, many rigid dicarboxylates^[7] have been employed as organic building blocks. As an illustration, bis(carboxylate) (e.g. terephthalate) was selected to design porous materials when engaged with either $\text{Zn}_4\text{O}^{[8]}$ or Cr_3O clusters.^[9] The isorecticular principle states that a variation of the length of the rigid precursor can be exploited to tune the size of the pores,^[10] whereas the introduction of some flexibility in the organic building block can prevent the formation of isotypic materials.^[11] Many MOFs have been synthesized from

rigid poly(carboxylic acid) precursors; thus, the use of rigid phosphonic acid group represents also a great potential for the construction of hybrid materials. 1,4-Benzenediphosphonic acid or 4,4'-biphenyldiphosphonic acid^[12] were the first rigid diphosphonic acids employed for the synthesis of hybrid materials. More recently, 3D hybrid materials were formed starting from the rigid 3,5-diphosphonophenylphosphonic acid,^[13] BINOL–diphosphonic acid,^[14] or a rigid dendritic tetraphosphonic acid.^[15] In the last two cases, microporous materials were formed. Finally, the use of rigid heterobifunctional organic building blocks has been employed few times to form new hybrids. In these recent works the metallic partner was calcium^[16] or zinc^[17] and the organic precursor was *para*-phosphonobenzoic acid or 5-phosphonobenzene-1,3-dicarboxylic acid.

In this paper, we report the use of a heterobifunctional organic precursor [3-phosphonobenzoic acid (**2**)] possessing a rigid structure to synthesize hybrid materials involving three different types of metallic precursors (Mn, Co and Zn salts). We have investigated different conditions of synthesis (e.g., variation of the pH), which control the number of functional groups of the organic component linked to the inorganic networks.

Results and Discussion

Organic precursor **2** (Scheme 1) is readily synthesized in multigram quantities starting from commercial 3-bromobenzoic acid. First, the methyl ester was synthesized following the classical method of esterification. Then, methyl 3-

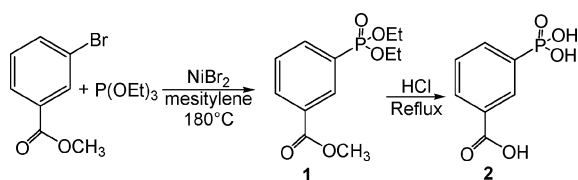
[a] Laboratoire CRISMAT, CNRS UMR 6508, ENSICAEN, 6 Blvd. Maréchal Juin, 14050 Caen Cedex, France
Fax: +33-2-31-95-16-00
E-mail: jean-michel.rueff@ensicaen.fr

[b] Laboratoire de Chimie Moléculaire et Thio-organique, ENSICAEN, Université de Caen Basse-Normandie, CNRS, 6 Blvd. Maréchal Juin, 14050 Caen, France

[c] Laboratoire CEMCA, CNRS UMR 6521, Université de Bretagne Occidentale, 6 Avenue Le Gorgeu, 29238 Brest, France
Fax: +33-2-98-01-70-01
E-mail: pjaffres@univ-brest.fr

Supporting information for this article is available on the WWW under <http://www.eurjic.org> or from the author.

(diethoxyphosphoryl)benzoate (**1**) was obtained by a modified Tav's method for the phosphonation of a halogenoaromatic substrate. This reaction takes place at a temperature higher than 180 °C by treating 3-bromobenzoate with triethylphosphite in the presence of a catalytic amount of nickel bromide. It must be noted that this reaction must be carried out with care. Indeed, the addition rate of triethylphosphite must be slow, especially at the beginning, because an induction period is observed, which is followed by an exothermic reaction. After purification by distillation, compound **1** was isolated in a yield ranging from 70 to 85%. In the last step, the ester functional groups were hydrolyzed by heating compound **1** at reflux in the presence of concentrated HCl. Compound **2** was isolated without further purification in a quasiquantitative yield.



Scheme 1. Synthetic pathway for compound **2**.

Single crystals of compound **2** were isolated and characterized by single-crystal X-ray diffraction (Table 3 and Supporting Information). The peculiar arrangement of the functional -COOH and -H₂PO₃ groups in the *meta* position of the benzene ring can be clearly identified. In the crystal structure, H₂PO₃C₆H₄CO₂H molecules form slices, shifted by 1/2 along the *c* axis and stacked along the *b* axis (see Figure 1b). As shown in Figure 1a, within these slices, molecules are linked together two by two through their functional -COOH groups. Molecules are packed to have the -COOH functionalities in a face-to-face position forming hydrogen bonds (intermolecular O–H distances close to 1.6 Å; encircled in Figure 1b). The juxtaposition of these supramolecular dimeric units leads to the formation of ribbons along the *c* direction. A more complex hydrogen-bonding scheme can be evidenced between the -H₂PO₃ groups, which ensures the cohesion of the global structure linking both the ribbons and slices together. Let us call –, 0 and + the ribbon as a function of their position along *a* (Figure 1b). The 0 ribbon of one slice is linked to the + and – ribbons of the adjacent slices through strong hydrogen bonds acting between the -H₂PO₃ groups (intermolecular O–H distances close to 1.6 Å); these O–H bonds are schematized and encircled in Figure 1a. This strong entwined supramolecular boundary results in the 3D character observed for the material.

Rigid bifunctional organic precursor **2** was used as a reagent in a hydrothermal synthesis in association with three different metallic salts. Because the pH of the reaction medium can have a great influence on the nature of the species present in solution and therefore an influence on the structure of the hybrid materials formed, the pH of the solutions were measured before the closure of the autoclaves and at their opening as reported in Table 1. Most of the reactions

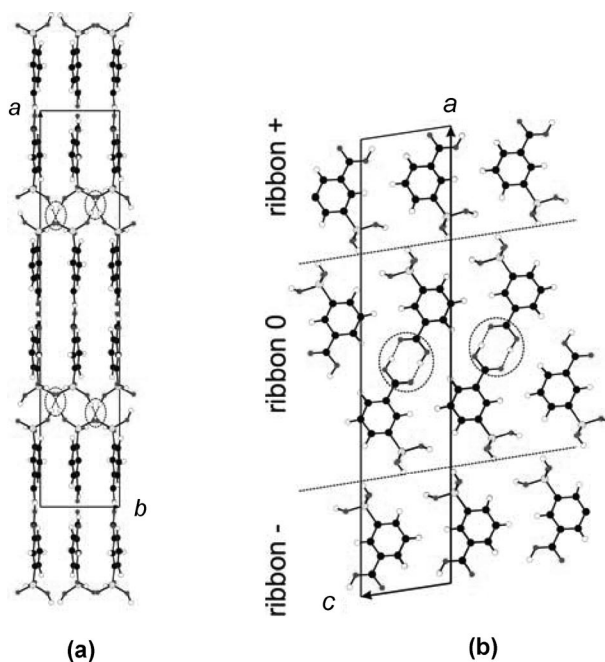


Figure 1. (a) Projection along *c* of the crystal structure of **2**. Dashed lines symbolized O–H hydrogen bonds. (b) Projection along *b* of the slices located around $y = 1/2$.

were repeated with the addition of urea, which, as reported in Table 1, increased the final pH of the solution. According to these conditions of synthesis, three crystal structures (compounds **3**, **4**, **6**) were resolved from single-crystal diffraction studies and one structure (compound **5**) from powder diffraction. Of note, the powder X-ray diffraction analyses of the solid recovered after the hydrothermal treatment point out that the products were phase pure.

Table 1. Summary of the hydrothermal syntheses of materials **3–6**. The syntheses were carried out with compound **2** (0.1 g, 0.49 mmol) in water (15 mL) heating at 160 °C for 40 h.

Entry	Inorganic Precursor (1.5 equiv.) ^[a]	Urea [equiv.]	Initial pH ^[b]	Final pH ^[c]	Material ^[d]	CN ^[e]
1	MnCl ₂	1.5	1.7	5.7	Mn(H ₂ O)(LH)	3
2	Mn(OAc) ₂	1.5	4.3	5.7	Mn(H ₂ O)(LH)	3
3	Mn(OAc) ₂	none	4.3	4.1	Mn(H ₂ O)(LH)	3
4	Co(NO ₃) ₂	1.5	1.7	6.2	Co(H ₂ O)(LH)	4
5	Co(OAc) ₂	1.5	4.4	6.2	Co(H ₂ O)(LH)	4
6	Co(OAc) ₂	none	4.3	3.9	Co(H ₂ O)(LH)	4
7	Zn(OAc) ₂	1.5	4.2	5.4	Zn ₃ (H ₂ O) ₂ (LH) ₂	6
8	Zn(OAc) ₂	none	4.1	4.1	Zn(H ₂ O)(LH)	5

[a] MnCl₂ = MnCl₂·4H₂O; Mn(OAc)₂ = Mn(CH₃COO)₂·2H₂O; Co(NO₃)₂ = Co(NO₃)₂·6H₂O; Co(OAc)₂ = Co(CH₃COO)₂·4H₂O; Zn(OAc)₂ = Zn(CH₃COO)₂·2H₂O. [b] Measured 15 min after stirring the substrates in water. [c] Measured at the opening of the pressured vessel. [d] LH = PO₃C₆H₄CO₂H. [e] CN = Compound number.

Table 3 summarizes the crystal parameters and the data used for the structure refinements of compounds **2**, **3**, **4**, **5** and **6**. The unit cell volumes of the isotypic compounds (**3**, **4** and **5**) with Mn to Zn decrease from 918.42 to 884.25 Å³ in accordance with the contraction of the radii of the transi-

tion element of the same row when the atomic number increases. These compounds consist of inorganic layers interleaved regularly with organic layers (Figure 2). The organic part is characterized by the presence of supramolecular dimeric units involving two carboxylic acid groups bearing by two molecules covalently bonded to two distinct inorganic layers. In materials **3** and **4**, the Mn^{2+} or Co^{2+} ions are bonded to the oxygen atoms of the phosphonate groups. The polyhedra of coordination around the transition elements are completed with water molecules in order to form an octahedron of oxygen atoms around each transition metal. This octahedron is distorted and the deformation varies according to the nature of the divalent ion; for Co^{2+} there are five bonds shorter than 2 \AA and a long one of 2.408 \AA , for Mn^{2+} three short bonds around 2.12 \AA , two medium bonds around 2.21 \AA and one very long bond of 2.505 \AA are observed.

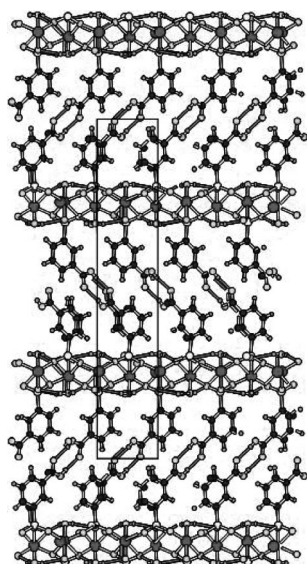


Figure 2. Projection of the structure of $\text{M}(\text{H}_2\text{O})(\text{PO}_3\text{C}_6\text{H}_4\text{CO}_2\text{H})$ along the a axis (**3**, $\text{M} = \text{Mn}$; **4**, $\text{M} = \text{Co}$; **5**, $\text{M} = \text{Zn}$).

The structure of material **5** ($\text{M} = \text{Zn}$) was obtained from powder X-ray diffraction study (Figure 3). In material **5**, which is isostructural with materials **3** and **4**, the coordination of Zn^{2+} is similar to the cobalt ones with five short distances and one very long one. The phosphorus atoms are surrounded by three oxygen atoms and one carbon atom that form a tetrahedron around it. In the structures of **3**, **4** and **5**, the octahedra share corners leading to a pseudoperovskite layer (Figure 4a). The PO_3C tetrahedra share one edge with the MO_6 octahedra leading to MPO_7C and one corner with another octahedron (Figure 4b). This arrangement is similar to the VPO_8 units seen in the $\text{Li}_2\text{VO}_2\text{PO}_4$ frameworks or within the layers of $\text{M}^{\text{II}}(\text{RPO}_3) \cdot \text{H}_2\text{O}$ series reported in the literature.^[18]

This latter bonding distorts the perovskite layer by a drastic tilt of the octahedra versus the plane containing the metals. Following the nomenclature proposed by Cheetham, Rao and Feller^[1] to describe the dimensionality of

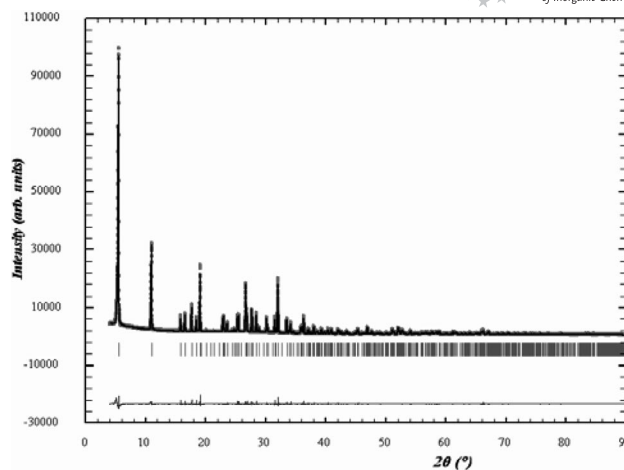


Figure 3. X-ray diffraction data recorded on powder from $\text{Zn}(\text{H}_2\text{O})(\text{PO}_3\text{C}_6\text{H}_4\text{CO}_2\text{H})$ (**5**). The vertical dashes correspond to the calculated position of the peaks, the bottom line to the difference between experimental and calculated pattern.

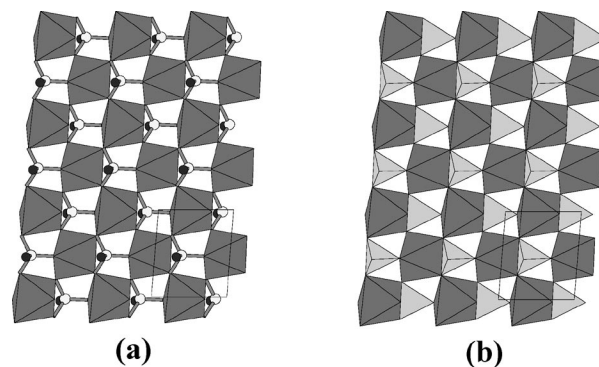


Figure 4. (a) The pseudoperovskite layer; (b) view of the $[\text{M}^{2+}\text{PO}_6\text{C}]_{\infty}$ layer.

hybrid materials, compounds **3**, **4** and **5** are 2D with regard to the inorganic (I^2) part owing to the infinite metal–oxygen–metal networks in two directions (ac planes). Along to the c axis, the organic molecules are bonded together through supramolecular links. Regarding the stability and the role of these supramolecular links to explain the packing of materials **3**, **4** and **5**, we conclude that the hydrogen bonds have a crucial role in describing the global dimensionality of these materials (Table 2). The organic molecules are bonded together (supramolecular link) along the b direction, which is orthogonal to those involved describing the inorganic networks. Therefore, the organic part is 1D. Materials **3**, **4** and **5** can therefore be classified in the category I^2O^1 , which corresponds to 3D materials. It should be noted that compound **5** can also be obtained without hydrothermal treatment by stirring an aqueous solution of **2** with Zn^{II} acetate salt at room temperature. Following this procedure, a microcrystalline powder is obtained. Syntheses performed in aqueous solution at room temperature with Mn^{II} and Co^{II} acetate salts and compound **2** do not result in materials **3** and **4**. However, when the mother solution is

Table 2. The hydrogen-bonding networks in **2**, **3** and **4**.

$\text{H}_2\text{PO}_3\text{C}_6\text{H}_4\text{CO}_2\text{H}$ (2)			
O11–H11 1.00(1) Å	H11...O22 1.55(1) Å	O11–H11...O22 173(1)°	O11...O22 2.541(4) Å
O13–H12 0.97(1) Å	H12...O12 1.62(1) Å	O13–H12...O12 175(1)°	O13...O12 2.594(5) Å
O15–H17 0.98(1) Å	H17...O14 1.66(1) Å	O15–H17...O14 172(1)°	O15...O14 2.627(4) Å
O21–H21 0.94(1) Å	H21...O22 1.63(1) Å	O21–H21...O22 172(1)°	O21...O22 2.570(4) Å
O23–H22 1.08(1) Å	H22...O12 1.47(1) Å	O23–H22...O12 176(1)°	O23...O12 2.543(5) Å
O24–H27 1.00(1) Å	H27...O25 1.62(1) Å	O24–H27...O25 180(1)°	O24...O25 2.624(4) Å
$\text{Mn}(\text{H}_2\text{O})(\text{PO}_3\text{C}_6\text{H}_4\text{CO}_2\text{H})$ (3)			
O6–H61 0.81(2) Å	H61...O1 2.21(2) Å	O6–H61...O1 138(1)°	O6...O1 2.871(1) Å
O6–H62 0.86(2) Å	H62...O2 2.03(2) Å	O6–H62...O2 167(2)°	O6...O2 2.877(1) Å
O4–H41 0.79(3) Å	H41...O5 1.88(3) Å	O4–H41...O5 172(2)°	O4...O5 2.659(2) Å
$\text{Co}(\text{H}_2\text{O})(\text{PO}_3\text{C}_6\text{H}_4\text{CO}_2\text{H})$ (4)			
O6–H61 0.76(3) Å	H61...O1 2.19(3) Å	O6–H61...O1 147(3)°	O6...O1 2.856(1) Å
O6–H62 0.87(3) Å	H62...O2 2.07(3) Å	O6–H62...O2 166(3)°	O6...O2 2.924(1) Å
O4–H41 0.93(6) Å	H41...O5 1.77(6) Å	O4–H41...O5 167(5)°	O4...O5 2.677(3) Å

heated whilst stirring at 70 °C for several hours, material **3** is obtained as a light-brown precipitate with a yield of 40%. All our trials to obtain material **4** by this way were unfruitful.

Increasing the pH during the synthesis of **6** by the addition of urea in the course of the hydrothermal treatment (Table 1, Entry 7) leads to a framework very different from the three previous compounds owing to the ability of the Zn^{2+} ion to adopt other coordination than octahedral. All the oxygen atoms belonging to the phosphonate organic molecule are bonded to zinc atoms and three independent zinc ions are observed. The first one (Zn1) is tetrahedrally coordinated to oxygen atoms, which are also bonded to the phosphorus atoms of the phosphonates. The others (Zn2 and Zn3) are surrounded by five oxygen atoms forming a trigonal bipyramid: two oxygen atoms of the phosphonate group, two from the carboxylate group and one water molecule. The framework is made of inorganic columns surrounded by organic columns and vice versa (Figure 5).

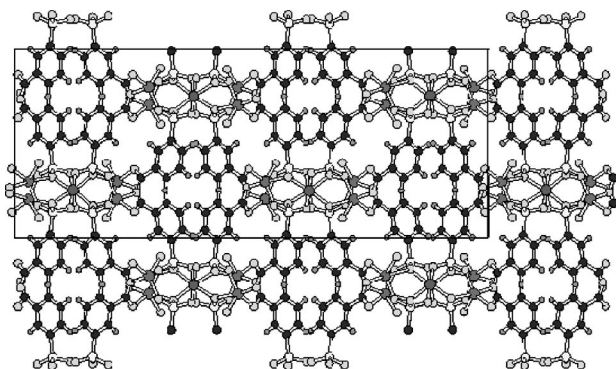


Figure 5. Projection along the *a* axis of the structure of $\text{Zn}_3\text{-(H}_2\text{O)}_2(\text{PO}_3\text{C}_6\text{H}_4\text{CO}_2)_2$ (**6**).

The inorganic columns running along the *a* axis are made of ZnO_5 bipyramids and ZnO_4 and PO_3C tetrahedral sharing corners (Figure 6a,b).

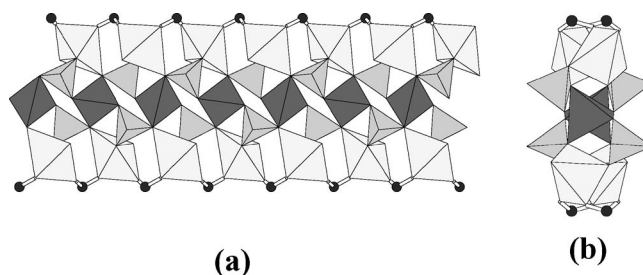


Figure 6. (a) The inorganic chain running along the *a* axis; (b) inorganic chain shown down the *a* axis.

The organic columns, also running along the *a* axis, are made of isolated phosphonate groups. In this structure, each molecule **2** is bonded to six zinc atoms (Figure 7). Regarding the dimensionality of compound **6**, the contribution of the inorganic network is one (I^1), as the inorganic part is composed of chains running along the *a* axis. These inorganic chains are bonded together with the organic molecules along the *b* direction, but also along the *c* axis. Therefore, the contribution of the organic part to the di-

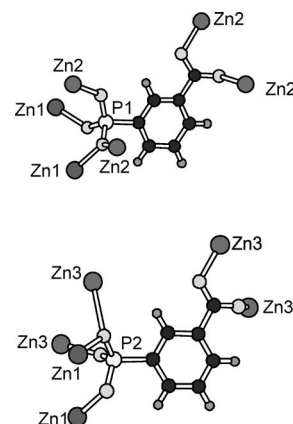


Figure 7. The surrounding of the two independent $\text{PO}_3\text{C}_6\text{H}_4\text{CO}_2$ molecules present in material **6**.

dimensionality of compound **6** is two. Hence, compound **6** can be classified in the category I^1O^2 forming a 3D structure. The contribution of organic part to the dimensionality of material **6** is increased compared to that of material **3** or **4**. Such organization can be explained by the linkage between the two functional groups present on organic precursor **2** and the inorganic part. Moreover, this 3D organization arises from the rigidity of the organic precursor, which is locked into a bent shape owing to the presence of the functional groups in the *meta* position on the aromatic ring.

From these structural studies we noticed that when Zn^{II} salts are engaged with organic molecule **2**, the pH of the reaction media has a remarkable effect on the structural organization of the hybrids formed. At low pH, compound **5** is formed exclusively, as only the phosphonic acid is linked to the inorganic network, whereas the carboxylic acids are engaged into a dimeric unit through hydrogen bonding. This observation can be justified by the fact that the phosphonic acid is first ionized in water due to its lower pK_a . Therefore, the phosphonate salt must have a greater reactivity with the metallic precursor in comparison to the carboxylic acid group. In contrast, when the pH of the reaction media increases during the hydrothermal synthesis by the transformation of urea into ammonia, the carboxylic acid is also deprotonated leading in that case to the formation of compound **6**, which is characterized by the implication of the two groups (phosphonic and carboxylic) in the inorganic network. Therefore, a pH dependent chemoselectivity is observed leading to the formation of materials **5** or **6**, which can be synthesized selectively. It is worth noting that the influence of the condition of reactions, including the addition of basic compounds, can modify the structure of the resulting materials.^[19] If the pH plays an important role in the case of the synthesis of material **5** and **6**, it appears to have no influence when cobalt or manganese salts are used as inorganic precursors. Indeed, even in presence of urea (Table 1, Entries 1, 2, 4 and 5), layered materials **3** or **4** are exclusively formed. The pH of the final solution can reach a value of 6.2 (Table 1, Entry 5) without any evidence for the formation of a phase in which the two functional groups would be linked to the inorganic network. The influence of the composition of the inorganic salt has also been studied, as the counter anion can have an influence on the pH of the reaction media. For instance, when $Co(NO_3)_2 \cdot 6H_2O$ (Table 1, Entry 4) or $Co(CH_3COO)_2 \cdot 4H_2O$ (Table 1, Entry 5) are used the initial pH, respectively 1.7 and 4.4, were noticeably different, whereas the final pH was identical (6.2). In both cases, the same layered material **4** is formed. Similar behaviour is observed when manganese salts are used (Table 1, Entries 1 and 2). Therefore, the chemoselectivity when Mn or Co salts are used is not pH dependent in the range of pH of 4 to 6.2.

The SEM characterizations (see Supporting Information) are consistent with the single X-ray structures of compounds **3**, **4**, **5** and **6**. Indeed, platelets of average size $50 \mu m \times 50 \mu m$ for **3**, $100 \mu m \times 100 \mu m$ for **4** and $2 \mu m \times 2 \mu m$ for **5** are observed by SEM. These characteristics are in good agreement with the existence of a layered structure for these

compounds. In contrast, compound **6** forms needles with an average size of $200 \mu m \times 50 \mu m$. This observation is consistent with the absence of a layered organization in this compound.

The thermogravimetric curves (see Supporting Information) of compounds **3**, **4**, **5** and **6** exhibit an initial mass loss between room temperature and $330 \text{ }^\circ\text{C}$, which is in good agreement with the departure of the coordinated water molecules present in the structure: 5.8% for one H_2O in $C_7H_7MnO_6P$ (theoretical loss: 6.6%), 7% for one H_2O in $C_7H_7CoO_6P$ (theoretical loss: 6.5%), 4.9% for two H_2O in $C_{14}H_{12}Zn_3O_{12}P_2$ (theoretical loss: 5.7%) and 6.4% for one H_2O in $C_7H_7ZnO_6P$ (theoretical loss: 6.3%). After this dehydration process, a series of several more mass losses are observed, which are attributed to the decomposition of the compound and the formation of $Mn_2P_2O_7$ for $C_7H_7MnO_6P$, $Co_2P_2O_7$ for $C_7H_7CoO_6P$, $Zn_3(PO_4)_2$ for $C_{14}H_{12}Zn_3O_{12}P_2$ and $Zn_2P_2O_7$ for $C_7H_7ZnO_6P$. These final materials were identified by X-ray diffraction and their formation is in good agreement with the total weight of loss: 44% for $C_7H_7MnO_6P$, 43% for $C_7H_7CoO_6P$, 40% for $C_{14}H_{12}Zn_3O_{12}P_2$ and 45% for $C_7H_7ZnO_6P$.

The IR spectra of materials **3**, **4**, **5** and **6** are depicted in Figure 8. The resemblance between the IR spectra of compounds **3**, **4** and **5** was expected in view of their structural similarities. The broad signal between 2500 and 3600 cm^{-1} and the strong peak around 1700 cm^{-1} are characteristic of the presence of the hydrogen bonds between the carboxylic acid groups, resulting from the dimeric carboxylic acid unit into the interlayer space. As expected, these signals are dramatically reduced in the IR spectra of material **6** owing to the absence of hydrogen bonds.

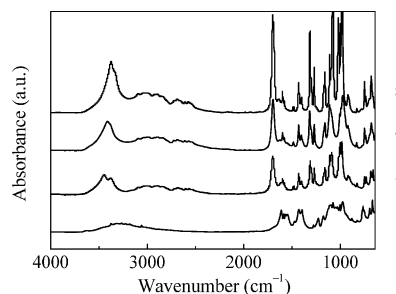


Figure 8. Infrared spectra of $Mn(H_2O)(PO_3C_6H_4COOH)$ (**3**), $Co(H_2O)(PO_3C_6H_4COOH)$ (**4**), $Zn(H_2O)(PO_3C_6H_4COOH)$ (**5**) and $Zn_3(H_2O)_2(PO_3C_6H_4COO)_2$ (**6**).

Magnetic measurements were performed with a SQUID magnetometer on an assembly of $Mn(H_2O)(PO_3C_6H_4COOH)$ and $Co(H_2O)(PO_3C_6H_4COOH)$ unoriented small crystals. In Figure 9, the magnetization is shown for both compounds.

A fitting by the Curie law gives that the Mn compound presents a moment of $5.97 \mu_B/Mn$ and an extrapolation temperature $\theta = -72 \text{ K}$ for a Neel temperature of $T_N = 22.5 \text{ K}$. The ratio $\theta/T_N \approx 3$ corresponds to 3 first Mn neighbours in the structure, which does not correspond to any physical neighbours. An alternative fitting procedure with a Fisher law^[20] (for 1D chains) modified to introduce

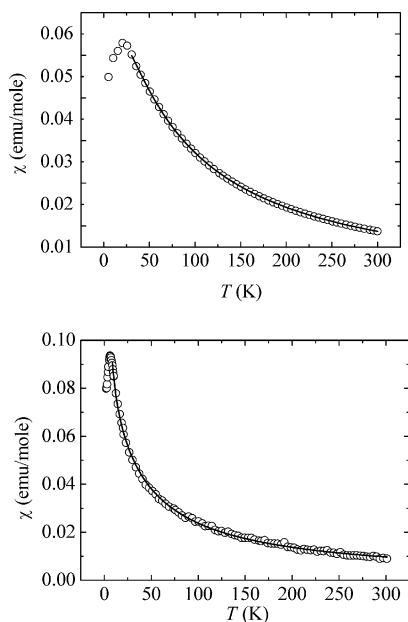


Figure 9. Magnetization vs. temperature obtained in zero field cooled process under 3000 G for $\text{Mn}(\text{H}_2\text{O})(\text{PO}_3\text{C}_6\text{H}_4\text{COOH})$ (top) and $\text{Co}(\text{H}_2\text{O})(\text{PO}_3\text{C}_6\text{H}_4\text{COOH})$ (bottom). The corresponding fitting parameters are given in the text.

an interchain coupling provides a smaller moment $5.40 \mu_{\text{B}}/\text{Mn}$ and an extrapolation temperature $\theta = -45 \text{ K}$ for a Neel temperature of $T_{\text{N}} = 22.5 \text{ K}$. The ratio θ/T_{N} corresponds to 2 first Mn neighbours within the chain, which seems reasonable. The smaller value of the moment can be due to the inappropriate extrapolation of this model. The values of about $5.97 \mu_{\text{B}}/\text{Mn}$ corresponds exactly to what is expected for $5/2$ moments of Mn^{2+} with no quench of L . The values of T_{N} , θ and μ_{B} are in good agreement with the values found in the literature for similar layered Mn^{2+} phosphonates (alkyl or phenyl).^[21,22] The isotopic cobalt compound presents a moment of $3.53 \mu_{\text{B}}$ and $T_{\text{N}} = 6.5 \text{ K}$, $\theta = -13 \text{ K}$. The ratio $\theta/T_{\text{N}} = 2$ confirms the isotopic character of the structures. The value of $3.53 \mu_{\text{B}}$ corresponds to fully quenched value of the L moment, which is classical for Co^{2+} . Slightly smaller than the value of μ_{B} described in the literature for Co^{2+} phenyl phosphonate, the difference can be easily explained by the temperature range used for the fitting model.^[20]

Conclusions

The use of rigid heterobifunctional compound **2** to design hybrid materials produces either I^2O^1 or I^1O^2 3D structures depending on the type of inorganic precursors involved and, in the case of Zn^{II} salt as inorganic source, the pH of the reaction media. When Mn or Co salts are employed (materials **3** and **4**), the single phosphonic acid group of compound **2** is engaged in the inorganic network, demonstrating the chemoselectivity of the hybrid construction. This construction is not pH dependent in the pH range studied. When Zn^{II} salt is used as inorganic source,

a pH dependent chemoselectivity is observed. At low pH, material **5**, isostructural with materials **3** and **4**, is formed. At higher pH, material **6** is formed in which both functional groups (phosphonic acid and carboxylic acid) are engaged in the inorganic network leading to a I^1O^2 3D network. The structure of this material is governed by the rigidity of organic building block **2**. This study illustrates that the use of a heterobifunctional organic precursor can produce materials in which carboxylic acid groups are not engaged with the inorganic networks, resulting in the obtained functional materials. Further studies are presently engaged to achieve postchemical transformations based on the reactivity of the carboxylic acid groups present in these materials. For instance, the introduction of amines in the interlayer space of compound **5** is presently studied. In contrast, with certain metallic precursors (Zn) and at controlled pH, rigid bifunctional organic precursor **2** can produce original hybrid structures.

Experimental Section

General: All compounds were fully characterized by ^1H , ^{13}C and ^{31}P NMR spectroscopy (Bruker AC 300 spectrometer). The following abbreviations were used: s singlet, d doublet, t triplet, q quadruplet, qt quintuplet, m multiplet. Mass spectra were recorded with a QTOF Micro (Waters), ionization electrospray positive (ESI), lockspray PEG, infusion introduction ($5 \mu\text{L}/\text{min}$), source temperature $80 \text{ }^\circ\text{C}$, desolvation temperature $120 \text{ }^\circ\text{C}$. Elemental analyses were recorded with an automatic apparatus CHNS-O ThermoQuest. Thermogravimetric analyses (TGA) were recorded at the rate of $2 \text{ }^\circ\text{C}/\text{min}$ from room temperature to $700 \text{ }^\circ\text{C}$ in air or under an atmosphere of nitrogen by using a SETARAM TGA 92 apparatus.

Methyl 3-(Diethoxyphosphoryl)benzoate (1): NiBr_2 (1.87 g; 8.55 mmol), methyl-3-bromobenzoate (23.00 g, 106.9 mmol) and mesitylene (16 mL) were placed under a nitrogen atmosphere in a two-necked, round-bottom flask fitted with a reflux condenser and an additional funnel. The suspension was heated at $180 \text{ }^\circ\text{C}$ and triethylphosphite (26.63 g, 160 mmol) was carefully added dropwise over 45 min. At the end of the addition, the solution was heated at $180 \text{ }^\circ\text{C}$ for 2 h. After cooling at room temperature, the volatiles, including the solvent, were removed in vacuo. Water (150 mL) was added to the residue, and the mixture was extracted with ethyl ether ($2 \times 75 \text{ mL}$). The organic phase was then washed with brine ($3 \times 40 \text{ mL}$), dried with MgSO_4 , filtered and concentrated in vacuo to produce an orange viscous oil. Purification by distillation under high vacuum (10 mTorr) was achieved in a Kugelrohr oven ($180 \text{ }^\circ\text{C}$), which produced a colourless viscous oil (23.27 g; 80% yield). ^1H NMR (300.13 MHz, CDCl_3): $\delta = 1.26$ (t, $^3J = 7.1 \text{ Hz}$, 6 H, $\text{CH}_3\text{CH}_2\text{O}$), 3.87 (s, O- CH_3), 3.95–4.18 (m, 4 H, $\text{CH}_2\text{-O-P}$), 7.49 (td, $^3J = 7.6 \text{ Hz}$, $^4J_{\text{HP}} = 4.0 \text{ Hz}$, CH^5), 7.94 (ddt, $^3J_{\text{HP}} = 12.9 \text{ Hz}$, $^3J = 7.6 \text{ Hz}$, $^4J = 1.3 \text{ Hz}$, CH^4), 8.15 (dq, $^3J = 7.8 \text{ Hz}$, $^4J_{\text{HH}} = ^5J_{\text{HP}} = 1.3 \text{ Hz}$, CH^6), 8.40 (dt, $^3J_{\text{HP}} = 13.7 \text{ Hz}$, $^4J = 1.3 \text{ Hz}$, CH^2) ppm. ^{31}P NMR (121.49 MHz, CDCl_3): $\delta = 18.10$ ppm. ^{13}C NMR (75.47 MHz, CDCl_3): $\delta = 16.22$ (d, $J = 6.4 \text{ Hz}$), 52.26 (s), 62.28 (d, $J = 5.5 \text{ Hz}$), 128.63 (d, $J = 6.4 \text{ Hz}$), 129.00 (d, $J = 165.1 \text{ Hz}$), 130.63 (d, $J = 9.5 \text{ Hz}$), 132.71 (d, $J = 10.9 \text{ Hz}$), 133.21 (d, $J = 3.0 \text{ Hz}$), 135.88 (d, $J = 10.0 \text{ Hz}$), 166.00 (d, $J = 2.0 \text{ Hz}$) ppm. HRMS (ESI-TOF): calcd. for $\text{C}_{12}\text{H}_{18}\text{O}_5\text{P} [\text{M} + \text{H}]^+$ 273.0892; found 273.0884.

3-Phosphonobenzoic Acid (2): Compound **1** (22.12 g; 81.25 mmol) and concentrated HCl (37% in water, 300 mL) were mixed, and the solution was heated at reflux for 21 h. The solution was concentrated in vacuo, and the resulting solid was dried in vacuo to produce **2** (16.05 g; 98% yield). Single crystals suitable for X-ray studies were directly isolated after a slow cooling of the acidic solution. ^1H NMR (300.13 MHz, D_2O): δ = 7.38 (m, CH^5), 7.77 (dd, $^3J_{\text{HP}}$ = 12 Hz, 3J = 7 Hz, CH^4), 7.89 (d, 3J = 8 Hz, CH^6), 8.10 (dd, $^3J_{\text{HP}}$ = 14 Hz, 4J = 1 Hz, CH^2) ppm. ^{31}P NMR (121.49 MHz, D_2O): δ = 14.81 ppm. ^{13}C NMR (75.47 MHz, D_2O): δ = 129.32 (d, J = 14.5 Hz), 130.9 (d, J = 14.8 Hz), 131.72 (d, J = 11.4 Hz), 132.30 (d, J = 184.0 Hz), 133.11 (d, J = 12.8 Hz), 135.51 (d, J = 10.5 Hz), 169.80 (s) ppm. $\text{C}_7\text{H}_7\text{O}_5\text{P}$ (202.1): calcd. C 41.60, H 3.49; found C 41.92, H 3.67. IR (KBr): $\tilde{\nu}$ = 3079, 2890, 2845, 2681, 2572, 2292, 1700, 1679, 1603, 1581, 1449, 1407, 1320, 1273, 1163, 1111, 1085, 1014, 956, 853, 829, 755, 734, 687, 661 cm^{-1} .

Preparation of $\text{Mn}(\text{H}_2\text{O})(\text{PO}_3\text{C}_6\text{H}_4\text{COOH})$ (3**) and $\text{Co}(\text{H}_2\text{O})(\text{PO}_3\text{C}_6\text{H}_4\text{COOH})$ (**4**) by Hydrothermal Synthesis:** In a 50-mL PTFE insert was dissolved 3-phosphonobenzoic acid (0.2 g, 0.98 mmol, 1 equiv.) in permuted water (15 mL). To this solution was added the desired transition metal salt [1.5 equiv.; $\text{MnCl}_2 \cdot 4\text{H}_2\text{O}$ (0.294 g, 1.48 mmol) for **3** or $\text{Co}(\text{NO}_3)_2 \cdot 6\text{H}_2\text{O}$ (0.432 g, 1.48 mmol) for **4**] and urea (0.089 g, 1.48 mmol, 1.5 equiv.). The insert was transferred into a Berghof pressure digestion vessel and heated from room temperature to 160 °C over 18 h and then further heated at 160 °C for 40 h and cooled to room temperature over 18 h. After filtration, the resulting compounds, obtained as light brown (for **3**) or purple (for **4**) crystallites, were washed with water, rinsed with absolute ethanol and dried in air.

Compound 3: Yield: 0.198 g (73%). IR (KBr): $\tilde{\nu}$ = 3448, 3378, 3095, 3003, 2894, 2852, 2686, 2602, 2567, 1699, 1598, 1583, 1483, 1428, 1403, 1311, 1269, 1158, 1109, 1091, 1002, 984, 920, 910, 827, 749, 732, 683, 659 cm^{-1} . TGA (under N_2): 5.8% weight loss at about 310 °C (6.6% of water calculated). $\text{C}_7\text{H}_7\text{MnO}_6\text{P}$ (273.04): calcd. C 30.79, H 2.58; found C 30.29, H 2.71.

Compound 4: Yield: 0.101 g (38%). IR (KBr): $\tilde{\nu}$ = 3412, 3379, 3092, 2990, 2895, 2855, 2723, 2690, 2611, 2573, 1697, 1627, 1599, 1584, 1486, 1431, 1404, 1317, 1270, 1159, 1111, 1005, 992, 975, 920, 831, 749, 736, 679 cm^{-1} . TGA (in air): 7% weight loss at about 195 °C (6.5% of water calculated). $\text{C}_7\text{H}_7\text{CoO}_6\text{P}$ (277.04): calcd. C 30.35, H 2.55; found C 30.33, H 2.69.

Preparation of Compound 3 by Soft Chemistry: An aqueous solution (30 mL) of 3-phosphonobenzoic acid (0.6 g, 2.96 mmol, 1 equiv.) was added to a stirred aqueous solution (20 mL) of $\text{Mn}(\text{CH}_3\text{COO})_2 \cdot 4\text{H}_2\text{O}$ (1.09 g, 4.47 mmol, 1.5 equiv.). The solution was stirred overnight. The white precipitate formed was filtered, washed with water, rinsed with absolute ethanol and dried in air. X-ray diffraction confirmed that the compound synthesized by this way has the same structure as that obtained by hydrothermal synthesis (0.66 g, 810% yield).

Preparation of $\text{Zn}(\text{H}_2\text{O})(\text{PO}_3\text{C}_6\text{H}_4\text{COOH})$ (5**) Hydrothermal Synthesis:** In a 50-mL PTFE insert was dissolved 3-phosphonobenzoic acid (0.1 g, 0.49 mmol, 1 equiv.) in distilled water (15 mL). To this solution was added $\text{Zn}(\text{CH}_3\text{COO})_2 \cdot 2\text{H}_2\text{O}$ (0.162 g, 1.48 mmol, 1.5 equiv.). The insert was transferred into a Berghof pressure digestion vessel and heated from room temperature to 160 °C over 18 h and then further heated at 160 °C for 40 h and cooled to room temperature over 18 h. After filtration, the resulting compound obtained as a white powder was washed with water, rinsed with absolute ethanol and dried in air (0.095 g, 68% yield).

Preparation of Compound 5 by Soft Chemistry: An aqueous solution (30 mL) of 3-phosphonobenzoic acid (0.3 g, 1.48 mmol,

1 equiv.) was added dropwise to a stirred aqueous solution (60 mL) of $\text{Zn}(\text{CH}_3\text{COO})_2 \cdot 2\text{H}_2\text{O}$ (0.488 g, 2.22 mmol, 1.5 equiv.). After 30 min, a white precipitate started to be formed. The solution was stirred for 3 d, and the precipitate was then recovered by filtration, washed with water, rinsed with absolute ethanol and dried in air. X-ray diffraction confirmed that the compound synthesized by this way has the same structure as that obtained by hydrothermal synthesis (0.385 g, 91% yield). IR (KBr): $\tilde{\nu}$ = 3374, 3340, 3093, 3006, 2898, 2855, 2690, 2609, 2573, 1698, 1635, 1599, 1584, 1484, 1430, 1403, 1314, 1270, 1159, 1109, 1077, 1018, 1000, 979, 920, 912, 829, 779, 749, 735, 679 cm^{-1} . TGA (in air): 6.5% weight loss at about 250 °C (6.3% of water calculated). $\text{C}_7\text{H}_7\text{O}_6\text{PZn}$ (283.48): calcd. C 29.66, H 2.49; found C 29.21, H 3.0.

Preparation of $\text{Zn}_3(\text{H}_2\text{O})_2(\text{PO}_3\text{C}_6\text{H}_4\text{COO})_2$ (6**):** In a 50-mL PTFE insert was dissolved 3-phosphonobenzoic acid (0.2 g, 0.98 mmol, 1 equiv.) in permuted water (15 mL). To this solution was added $\text{Zn}(\text{CH}_3\text{COO})_2 \cdot 2\text{H}_2\text{O}$ (0.327 g, 1.48 mmol, 1.5 equiv.) and urea (0.089 g, 1.48 mmol, 1.5 equiv.). The insert was transferred into a Berghof pressure digestion vessel and heated from room temperature to 160 °C over 18 h and then further heated at 160 °C for 40 h and cooled to room temperature over 18 h. After filtration, the resulting compound obtained as white crystallites was washed with water, rinsed with absolute ethanol and dried in air (0.240 g, 86% yield). IR (KBr): $\tilde{\nu}$ = 3375, 3317, 3268, 3224, 3182, 3059, 1717, 1700, 1684, 1653, 1613, 1587, 1567, 1559, 1542, 1507, 1497, 1474, 1456, 1429, 1397, 1278, 1228, 1176, 1111, 1097, 1076, 1050, 1031, 1002, 975, 881, 825, 764, 754, 695, 667 cm^{-1} . TGA (in air): 4.9% weight loss at about 315 °C (5.7% of water calculated). $\text{C}_{14}\text{H}_{12}\text{O}_{12}\text{P}_2\text{Zn}_3$ (630.33): calcd. C 26.68, H 1.92; found C 26.64, H 2.44.

XRD Investigations: XRD investigation was performed by using Mo-K_α radiations on a K_α CCD (Bruker Nonius) diffractometer equipped with a CCD (charge coupled device) detector. Large Ω - and Φ -scans were used to both control the crystalline quality of different samples and determine the unit cell parameters. Single crystals of suitable size were then selected. Considering the cell parameters and the spot size (i.e. mosaicity) suitable data collection strategies have been defined. A scanning angle of 0.8° and a D_x (detector-sample distance) value of 34 mm were chosen; Φ - and Ω -scans were used. To collect a great number of weak reflections, but avoiding any detector saturation by reflections of strong intensity, different exposure times were used to collect the data. The diffracted intensities were collected up to $\theta = 40^\circ$. Following the symmetry of the crystal, one independent monoclinic or orthorhombic space was scanned. Plots of reciprocal lattice planes assembled from these series of experimental frames are sufficiently accurate to obtain an overall view of the reciprocal space. The conditions limiting the possible reflections were then observed and the possible space groups identified. The EvalCCD software^[23] was used to extract reflections from the collected frames and reflections were merged and rescaled as a function of the exposure time. Data were corrected from absorption by using the Sadabs program^[24] developed for scaling and correction of area detector data. Structural models were built up from Patterson map analysis (heavy atoms method) for **3**, **4** and **6** and with superflip^[25] by using charge-flipping methods for phase **2**. The model was subsequently introduced in the refinement program Jana2006,^[26] and all the atomic positions were refined and anisotropic atomic displacement parameters (ADP) were considered for all the atoms. At this step of the refinement, the hydrogen atoms can be located. The decreasing law of the diffusion factor as a function of $\sin\theta/\lambda$ implies that the main contribution of the hydrogen atoms to the diffracted intensity is condensed in the beginning of the diffraction patterns. Difference

Table 3. Summary of crystal data, intensity measurement and structure refinement for H₂PO₃C₆H₄CO₂H (2), [Mn(H₂O)(PO₃C₆H₄CO₂H)] (3), [Co(H₂O)(PO₃C₆H₄CO₂H)] (4), [Zn(H₂O)(PO₃C₆H₄CO₂H)] (5) and [Zn₃(H₂O)₂(PO₃C₆H₄CO₂)₂] (6).

	2	3	4	5 ^[a]	6
Molecular formula	C ₇ H ₇ O ₅ P	C ₇ H ₇ O ₆ PMn	C ₇ H ₇ O ₆ PCo	C ₇ H ₇ O ₆ PZn	C ₁₄ H ₁₂ O ₁₂ P ₂ Zn ₃
Formula mass	202.10	273.04	277.03	283.48	630.33
Laue class	2/m	2/m	2/m	2/m	[mm]m
Space group	C2 (14)	P2 ₁ /n (14)	P2 ₁ /n (14)	P2 ₁ /n (14)	Pcan (60)
a [Å]	34.839(3)	4.9742(3)	4.9119(3)	4.8727(2)	7.7731(4)
b [Å]	6.9003(4)	31.9775(1)	32.316(5)	32.0216(2)	14.344(2)
c [Å]	6.9606(5)	5.7936(2)	5.7481(8)	5.6948(2)	36.246(8)
β [°]	98.557(7)	94.593(4)	93.859(9)	95.6714(4)	90.
Cell volume [Å ³]	654.69(16)	918.43(7)	910.35(15)	884.215(8)	4041.4(9)
Z	4	4	4	4	8
Density	1.622	1.974	2.0207	2.130	2.0712
μ [mm ⁻¹]	0.318	1.616	2.065		3.753
T _{min}	0.7771	0.7871	0.7766		0.7732
T _{max}	0.9409	0.9309	0.9440		0.9255
Measured reflections	16874	25611	9169	781	35122
Independent data	5426	16624	7419		16651
Independent data with [I < 3σ]	3564	3739	2935		3087
Temp. data collect. [°C]	21	21	21	21	21
Secondary extinction	–	0.006(8)	1.1(2)		0.006(2)
Number of variables	234	165	165		311
R(F _o)	0.054	0.0280	0.0321	0.069	0.0622
R _w	0.043	0.0291	0.0363		0.0678

[a] Data from powder diffraction (see Figure 3).

Fourier series were then performed in the $0 \leq \sin\theta/\lambda \leq 0.5$ interval. The analysis of the observed maxima of density allowed the location of all the hydrogen atoms. The atomic position of the hydrogen atoms were refined but their ADP were considered as isotropic and fixed to 0.038 Å². The FullProf program^[27] was used to refine the structure of compound 5. The sample was loaded in a thin capillary ($\varnothing = 0.3$ mm) to avoid preferential orientation, and the data were registered with a Bruker D8 diffractometer up to 90° (2θ) by using the Cu-K_{α1} wavelength. Bond length constraints were applied on the organic moiety during the refinement. The final reliability factors were: R_{WP} = 5.34%, R_{EXP} = 2.64% ($\chi^2 = 4.04$) and R_{Bragg} = 8.05%. Table 3 summarizes the structure refinement data for compounds 2, 3, 4, 5 and 6

CCDC-686731 (for 4), -686732 (for 3), -686733 (for 6), -686734 (for 2) and -686735 (for 5) contain the supplementary crystallographic data for this paper. These data can be obtained free of charge from The Cambridge Crystallographic Data Centre via www.ccdc.cam.ac.uk/data_request/cif.

Supporting Information (see footnote on the first page of this article): Molecular structure of H₂PO₃C₆H₄CO₂H in the solid state; SEM characterization of compounds 3, 4, 5 and 6; TGA curves of 3, 4, 5 and 6.

Acknowledgments

The authors would like to thank Ms. Hélène Rousselière and Dr. Alain Pautrat from the Laboratoire de Cristallographie et Science des Matériaux, Caen, France, for their precious help. We thank the Service de RMN, UFR Sciences et Techniques, Université de Bretagne Occidentale, Brest for recording the NMR spectroscopic data.

[1] A. K. Cheetham, C. N. R. Rao, R. K. Feller, *Chem. Commun.* **2006**, 46, 4780–4795.

- [2] a) J. L. C. Rowsell, A. R. Millard, K. S. Park, O. M. Yaghi, *J. Am. Chem. Soc.* **2004**, 126, 5666–5667; b) R. E. Morris, P. A. Wheatley, *Angew. Chem. Int. Ed.* **2008**, 47, 4966–4981; c) G. Férey, *Chem. Soc. Rev.* **2008**, 37, 191–214.
- [3] P. M. Forster, A. K. Cheetham, *Top. Catal.* **2003**, 24, 79–86.
- [4] D. Bradshaw, T. J. Prior, E. J. Cussen, J. B. Claridge, M. J. Rosseinsky, *J. Am. Chem. Soc.* **2004**, 126, 6106–6114.
- [5] O. R. Evans, W. B. Lin, *Acc. Chem. Res.* **2002**, 35, 511–522.
- [6] P. Horcajada, C. Serre, M. Vallet-Regi, M. Sebban, F. Taulelle, G. Férey, *Angew. Chem. Int. Ed.* **2006**, 45, 5974–5978.
- [7] a) N. L. Rosi, J. Kim, M. Eddaoudi, B. Chen, M. O’Keeffe, O. M. Yaghi, *J. Am. Chem. Soc.* **2005**, 127, 1504–1518; b) P. Rabu, J.-M. Rueff, Z. L. Huang, S. Angelov, J. Souletie, M. Drillon, *Polyhedron* **2001**, 20, 1677–1685; c) N. Guillo, C. Livage, G. Férey, *Eur. J. Inorg. Chem.* **2006**, 24, 4963–4978.
- [8] H. Li, M. Eddaoudi, M. O’Keeffe, O. M. Yaghi, *Nature* **1999**, 402, 276–279.
- [9] G. Férey, C. Mellot-Draznieks, C. Serre, F. Millange, J. Dutour, S. Surblé, I. Margiolake, *Science* **2005**, 309, 2040–2042.
- [10] M. Eddaoudi, D. B. Moler, H. Li, B. Chen, T. M. Reineke, M. O’Keeffe, O. M. Yaghi, *Acc. Chem. Res.* **2001**, 34, 319–330.
- [11] T. Devis, O. Davis, M. Valls, J. Marrot, F. Couty, G. Férey, *J. Am. Chem. Soc.* **2007**, 129, 12614–12615.
- [12] G. Alberti, U. Costantino, F. Marmottini, R. Vivani, P. Zappelli, *Angew. Chem. Int. Ed. Engl.* **1993**, 32, 1357–1359.
- [13] a) D. J. Kong, J. Zon, A. McBee, A. Clearfield, *Inorg. Chem.* **2006**, 45, 977–986; b) G. B. Hix, V. Caignaert, J.-M. Rueff, L. Le Pluart, J. E. Warren, P. A. Jaffrès, *Cryst. Growth Des.* **2007**, 7, 208–211.
- [14] A. Hu, H. W. Ngo, W. Lin, *J. Am. Chem. Soc.* **2003**, 125, 11490–11491.
- [15] a) M. V. Vasylyev, E. J. Wachtel, R. Popovitz-Biro, R. Neumann, *Chem. Eur. J.* **2006**, 12, 3507–3514; b) J. M. Taylor, A. H. Mahmoudkhani, G. K. H. Shimizu, *Angew. Chem. Int. Ed.* **2007**, 46, 795–798; c) M. Vasylyev, R. Neumann, *Chem. Mater.* **2006**, 18, 2781–2783.
- [16] a) J. Svoboda, V. Zima, L. Benes, K. Melanova, M. Vlcek, *Inorg. Chem.* **2005**, 44, 9968–9976; b) S. Bauer, N. Stock, *J. Solid State Chem.* **2007**, 180, 3111–3120.

- [17] Z. Chen, Y. Zhou, L. Wenig, C. Yuan, D. Zhao, *Chem. Asian J.* **2007**, *2*, 1549–1554.
- [18] a) G. Cao, H. Lee, V. M. Lynch, T. Mallouk, *Inorg. Chem.* **1988**, *27*, 2781–2785; b) K. J. Martin, P. J. Squattrito, A. Clearfield, *Inorg. Chim. Acta* **1989**, *155*, 7–9.
- [19] S. Drumel, P. Janvier, P. Bardoux, M. Bujoli-Doeuff, B. Bujoli, *Inorg. Chem.* **1995**, *34*, 148–156.
- [20] J. C. Bonner, M. E. Fisher, *Phys. Rev.* **1964**, *135*, *3A*, A640–658.
- [21] S. G. Carling, P. Day, D. Visser, R. K. Kremer, *J. Solid State Chem.* **1993**, *106*, 111–119.
- [22] J. Le Bideau, C. Payen, B. Bujoli, P. Palvadeau, J. Rouxel, *J. Magn. Magn. Mater.* **1995**, *140–144*, 179–1720.
- [23] A. J. M. Duisenberg, *EvalCCD Thesis*, University of Utrecht, The Netherlands, **1998**.
- [24] G. M. Sheldrick, *SADABS: Program for Empirical Absorption Correction of Area Detector Data*, University of Göttingen, Germany, **1996**.
- [25] L. Palatinus, G. Chapuis, *J. Appl. Crystallogr.* **2007**, *40*, 786–790.
- [26] V. Petricek, M. Dusek, L. Palatinus, *Jana2006: Structure Determination Software Programs*, Institute of Physics, Praha, Czech Republic, **2006**.
- [27] J. Rodriguez-Carvajal, *Phys. B* **1993**, *192*, 55–69.

Received: May 14, 2008
Published Online: August 5, 2008